

# Bimetallic Perthiocarbonate Complex of Cobalt: Synthesis, Structure and Bonding

Alaka Nanda Pradhan, Shivankan Mishra, Urminder Kaur, Bikram Keshari Rout, Jean-François Halet, and Sundargopal Ghosh

## SUPPORTING INFORMATION

### Table of contents

#### II. Experimental details

Scheme S1      Synthesis of the vanadium thiolate complexes **5** and **6**.

#### A. Supplementary Data

Figure S1      Molecular structure and labeling diagrams of **5** and **6**.

Figure S2      Molecular structure and labeling diagrams of **6**.

#### B. Spectroscopic Details

Figure S3      ESI-MS spectrum of **2**.

Figure S4       $^1\text{H}$  NMR spectrum of **2** in  $\text{CDCl}_3$ .

Figure S5       $^{13}\text{C}\{^1\text{H}\}$  NMR spectrum of **2** in  $\text{CDCl}_3$ .

Figure S6      IR spectrum of **2** in  $\text{CH}_2\text{Cl}_2$ .

Figure S7       $^{11}\text{B}\{^1\text{H}\}$  spectrum of *in-situ*  $\{\mathbf{1} + \text{CS}_2 + \text{PPh}_3\}$  reaction mixture in  $\text{CDCl}_3$ .

Figure S8       $^{31}\text{P}\{^1\text{H}\}$  spectrum of *in-situ*  $\{\mathbf{1} + \text{CS}_2 + \text{PPh}_3\}$  reaction mixture in  $\text{CDCl}_3$ .

#### II. Computational Data

Table S1      Calculated Co–Co bond distances ( $d_{\text{M–M}}$ ), M–S bond distances ( $d_{\text{M–S}}$ ), Co–S–Co bond angles ( $\angle \text{Co–S–Co}$ ), WBI indices of M–M bond, natural charges ( $q_{\text{M}}$  and  $q_{\text{S}}$ ), natural valence population ( $\text{Pop}$ ) and HOMO–LUMO energy gap ( $\Delta E_{\text{H–L}}$ ) of **2**.

Table S2      TD-DFT calculated energies (excitation energy (eV),  $\lambda_{\text{calc}}$  (nm)), oscillator strength ( $f$ ), and main composition of the first UV–vis electronic excitations for **2**. Experimental absorption wavelengths ( $\lambda_{\text{exp}}$ , nm) of **2** are given for comparison.

Figure S9      Absorption spectrum of **2** computed at the TD-DFT-B3LYP/Def2-TZVP level of theory ( $\epsilon$  in  $\text{LM}^{-1}\text{cm}^{-1}$ ).

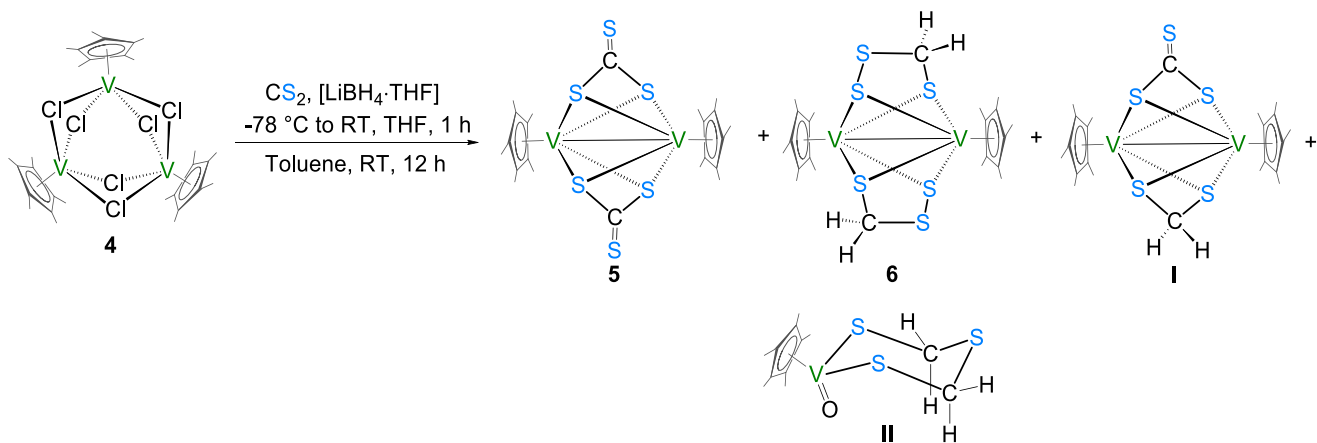
Figure S10      Selected molecular orbitals of **2** related to most intense electronic transitions [isocontour values:  $\pm 0.045 \text{ (e/bohr}^3\text{)}^{1/2}$ ].

### III. Cartesian Coordinates of the Optimized structure **2**

Figure S11      Optimized geometry of **2**.

### IV. References

## I. Experimental details



**Scheme S1.** Synthesis of the vanadium thiolate complexes **5** and **6**.

**Synthesis of 5 and 6.** In a pre-dried Schlenk tube,  $[\text{Cp}^*\text{VCl}_3]$  (**4**) (0.10 g, 0.13 mmol) was suspended in 10 mL toluene. To this suspension of **4**, a freshly prepared *in situ* intermediate from  $\text{CS}_2$  and  $[\text{LiBH}_4\cdot\text{THF}]$  was added dropwise at  $-78^\circ\text{C}$  under argon atmosphere. The reaction mixture was then kept under constant stirring at room temperature 18 hours. The solvent was removed under vacuum and the solid residue was extracted using *n*-hexane/THF (80:20 v/v) followed by separating and purifying through silica-gel coated TLC plates. Elution with *n*-hexane/toluene (80:20 v/v) yielded **5** and **6** (0.002 g, 4%) as a yellow solid along with the earlier reported yellow **I** (0.006 g, 12%) [1] and purple **II** (0.014 g, 11%) complexes [2].

## A. Supplementary Data

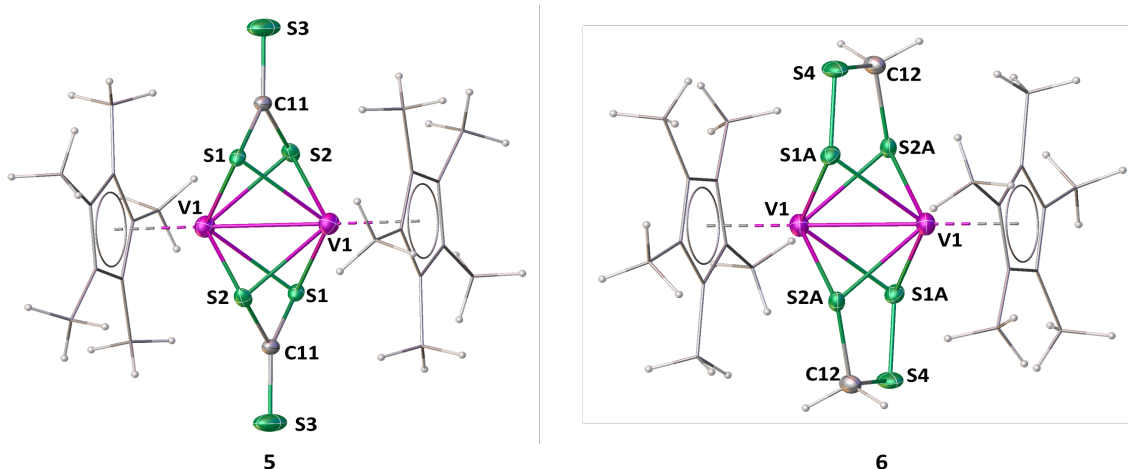


**Figure S1.** Molecular structure and labeling diagrams of **5** (left) and **6** (right) (co-crystallized in the same crystallographic unit). Selected bond lengths ( $\text{\AA}$ ) and bond angles ( $^\circ$ ): **5:**  $\text{V1-V1}$  2.570,  $\text{V1-S1}$  2.432(9),  $\text{V1-S1}$  2.438(8),  $\text{C11-S3}$  1.611(6),  $\text{C11-S2}$  1.792(13),  $\text{C11-S1}$  1.842(11),  $\text{S1-C11-S2}$  105.5(5),  $\text{V1-S1-V1}$  63.7(2),  $\text{V1-S2-V1}$  63.3(2),  $\text{S1-V1-S1}$  116.3(2),  $\text{S2-C11-S1}$  105.5(5),  $\text{C11-S1-V1}$  83.9(3),  $\text{C11-S2-V1}$  84.4(4). **6:**  $\text{V1-V1}$  2.570,  $\text{S1A-S4}$  1.805(18),  $\text{V1-S2A}$  2.43(2),  $\text{C12-S4}$  2.045 (17),  $\text{C12-S2A}$  1.80(3),  $\text{S1A-S4}$  1.805(18);  $\text{S2A-C12-S4}$  105.9(11),  $\text{S1A-S4-C12}$  102.5(9),  $\text{S4-S1A-V1}$  116.6(11),  $\text{V1-S1A-V1}$  62.4(6),  $\text{V1-S2A-V1}$  63.4(5).

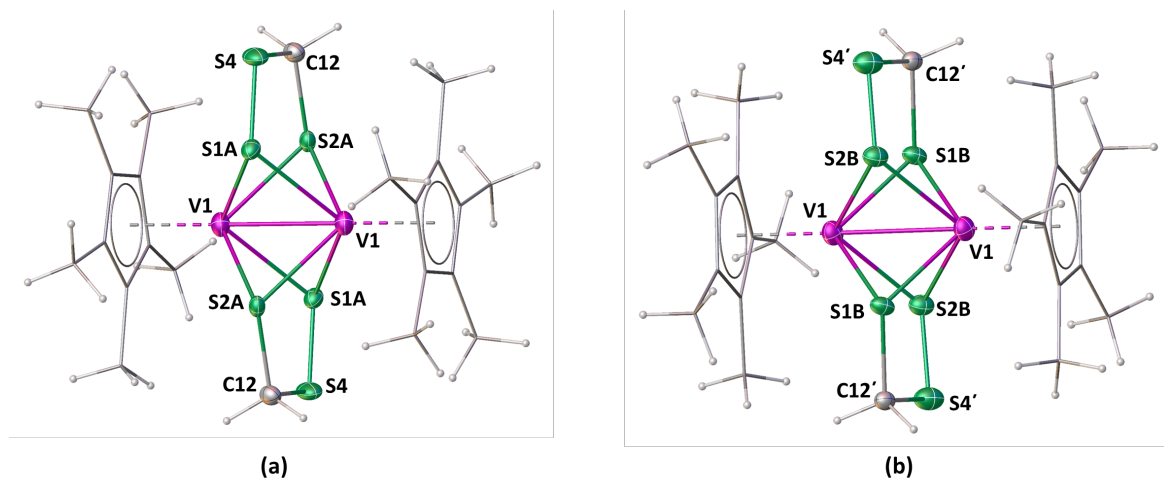


**Figure S2.** Molecular structure and labeling diagram of **6** with site occupancy ratio of (a):(b) = 0.31:0.13. Selected bond lengths ( $\text{\AA}$ ) and angles ( $^{\circ}$ ) are: (a): V1-S2A 2.43(2), C12-S4 2.045 (17), C12-S2A 1.80(3), S1A-S4 1.805(18); S2A-C12-S4 105.9(11), C12-S4-S1A 102.5(9); (b): V1-S2B 2.37(3), C12'-S4' 1.93 (4), C12'-S1B 1.84(5), S2B-S4' 1.80(2); S1B-C12'-S4' 106.0(3), C12'-S4'-S2B 102.0(18).

## I. Spectroscopic Details

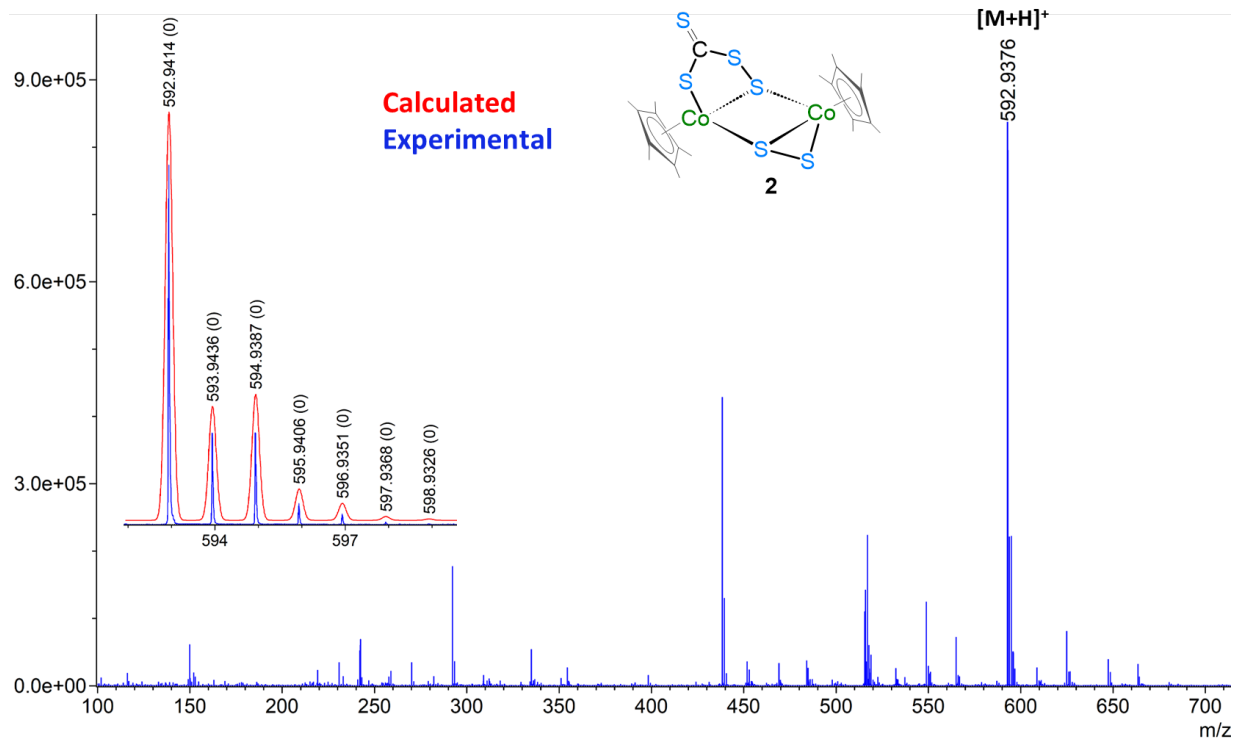


**Figure S3.** ESI-MS spectrum of **2**.

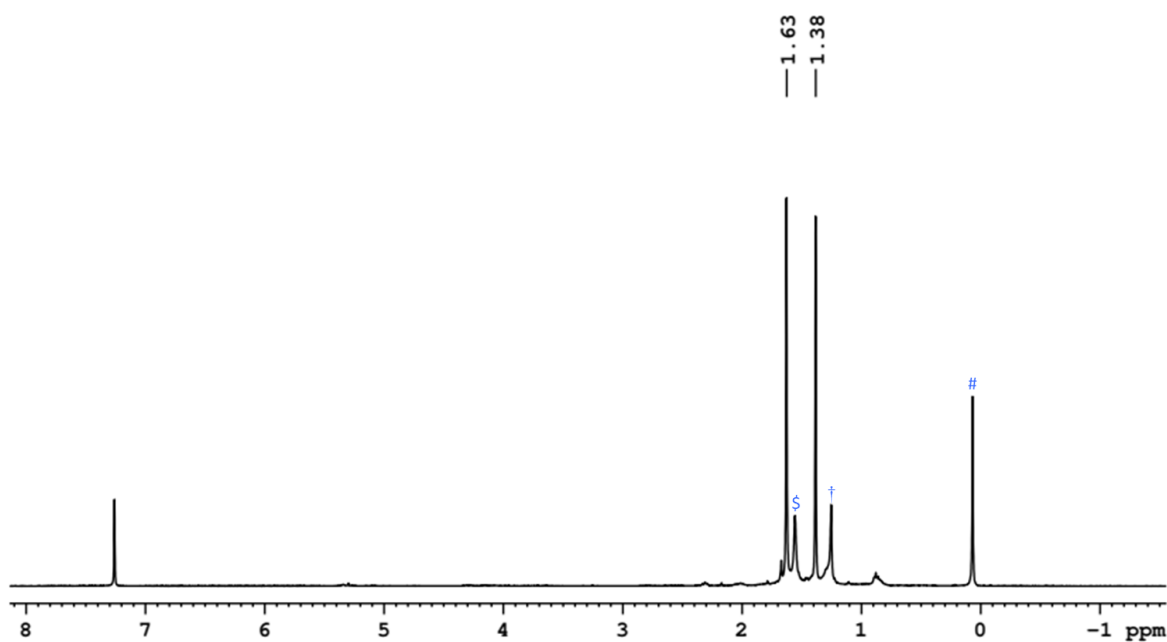


**Figure S4.**  $^1\text{H}$  NMR spectrum of **2** in  $\text{CDCl}_3$  (\$ $\text{H}_2\text{O}$ , †hexane, #silicone grease).

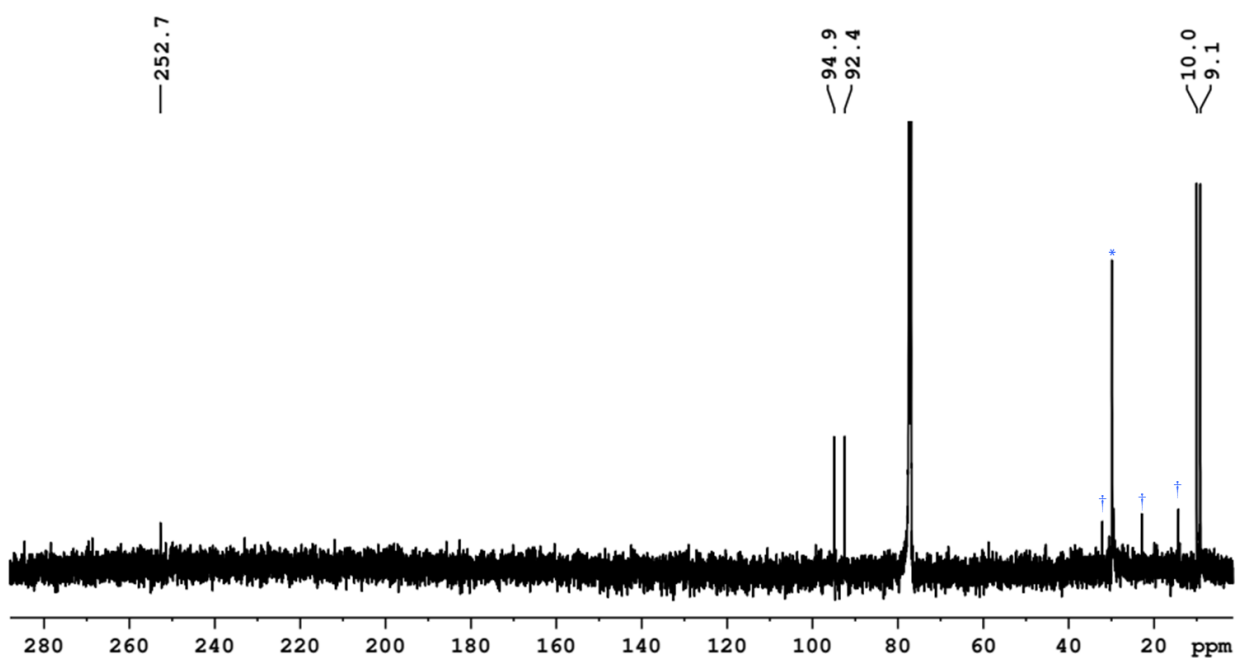


**Figure S5.**  $^{13}\text{C}\{^1\text{H}\}$  NMR spectrum of **2** in  $\text{CDCl}_3$  (†hexane, \*H-grease).

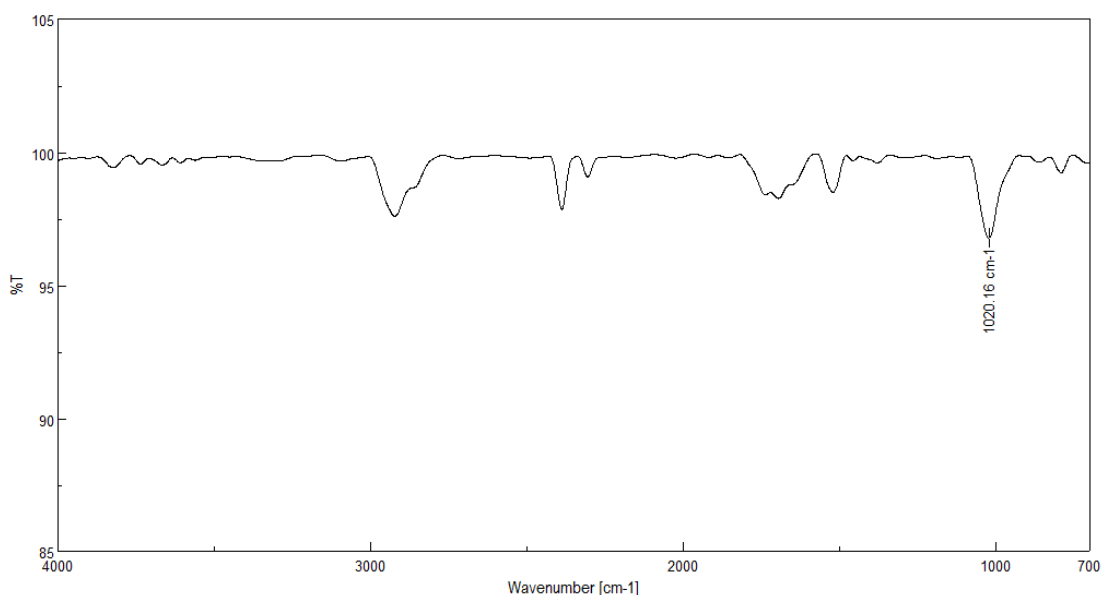


**Figure S6.** IR spectrum of **2** in  $\text{CH}_2\text{Cl}_2$ .

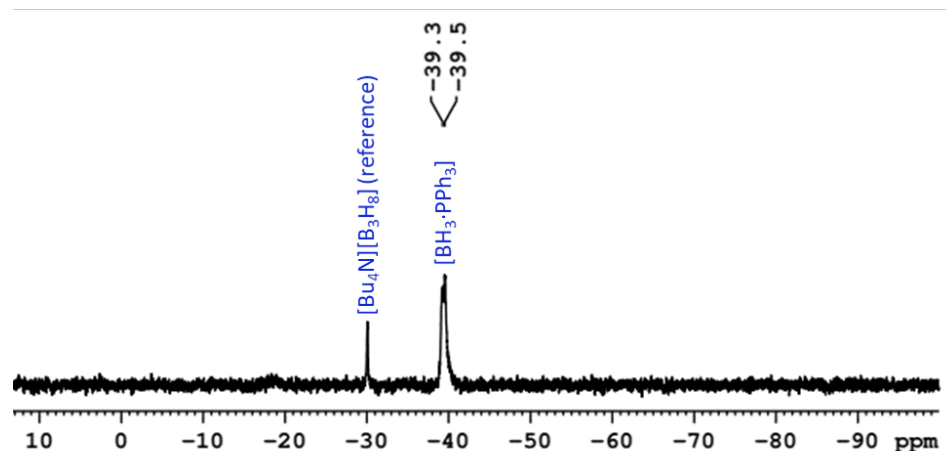


**Figure S7.**  $^{11}\text{B}\{^1\text{H}\}$  spectrum of *in-situ*  $\{\mathbf{1} + \text{CS}_2 + \text{PPh}_3\}$  reaction mixture in  $\text{CDCl}_3$ . [3-5]

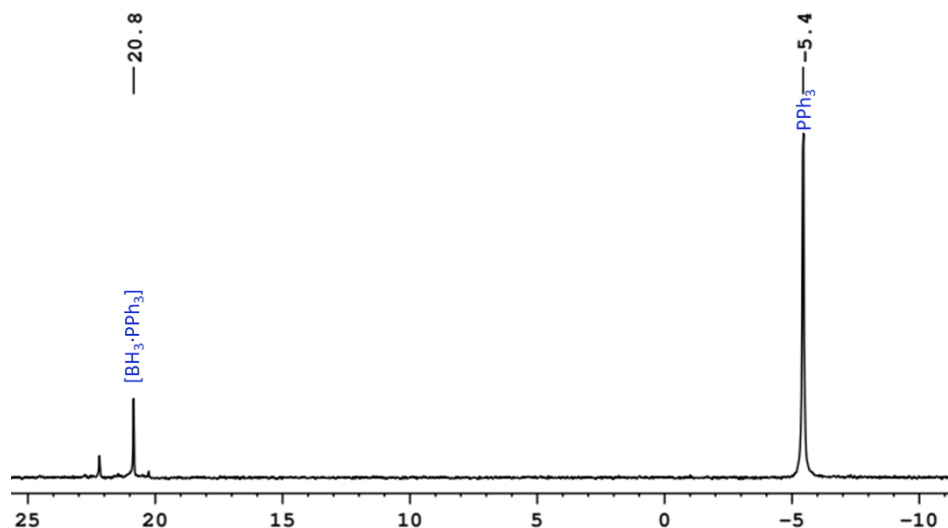


**Figure S8.**  $^{31}\text{P}\{^1\text{H}\}$  spectrum of *in-situ*  $\{\mathbf{1} + \text{CS}_2 + \text{PPh}_3\}$  reaction mixture in  $\text{CDCl}_3$ .

## II. Computational Data

**Table S1.** Calculated Co–Co bond distances ( $d_{\text{M–M}}$ ), M–S bond distances ( $d_{\text{M–S}}$ ), Co–S–Co bond angles ( $\angle \text{Co–S–Co}$ ), WBI indices of M–M bond, natural charges ( $q_{\text{M}}$  and  $q_{\text{S}}$ ), natural valence population ( $\text{Pop}$ ) and HOMO–LUMO energy gap ( $\Delta E_{\text{H–L}}$ ) of **2**.

$d_{\text{M–M}}$ (Å)	$d_{\text{M–S}}$ (Å)	$\angle \text{M–S–M}$ (°)	WBI (M–M)	$q_{\text{M}}$	$q_{\text{S}}$	$\text{Pop}$ (M <sub>val</sub> )	$\text{Pop}$ (S <sub>val</sub> )	$\Delta E_{\text{H–L}}$ (eV)
3.390	2.267	94.832		-0.454	-0.052	9.423	6.029	3.192
	2.283	97.317		-0.369	0.192	9.335	5.754	
	2.261				0.179		5.785	
	2.320				0.146		5.807	
	2.254				0.262		5.678	
	2.264				-0.153		6.110	

**Table S2.** TD-DFT calculated energies (excitation energy (eV),  $\lambda_{\text{calc}}$  (nm)), oscillator strength ( $f$ ), and main composition of the first UV–vis electronic excitations for **2**. Experimental absorption wavelengths ( $\lambda_{\text{exp}}$ , nm) of **2** are given for comparison.

No	Excitation Energy (eV)	Wavelength $\lambda$ (nm)		Main electronic transition (% weight) <sup>[b]</sup>
		Calc. ( $f$ ) <sup>[a]</sup>	Expt.	
1	2.229	556 (0.025)	570	HOMO→LUMO+3 (9)
2	2.782	446 (0.020)		HOMO-1→LUMO+1 (12)
3	2.816	440 (0.013)		HOMO-1→LUMO+3 (13)
4	2.907	427 (0.023)		HOMO-3→LUMO+1 (13)
				HOMO-1→LUMO+1 (13)
5	3.108	399 (0.023)		HOMO-2→LUMO+3 (12)
				HOMO-1→LUMO+3 (38)
6	3.126	397 (0.015)		HOMO-2→LUMO+2 (44)
7	3.248	382 (0.042)	384	HOMO-6→LUMO (11)
				HOMO-4→LUMO (12)
				HOMO-3→LUMO (15)
				HOMO-2→LUMO+4 (14)
8	3.400	365 (0.021)		HOMO-3→LUMO+1 (11)
				HOMO-3→LUMO+2 (11)

9	3.455	359 (0.019)	HOMO-5→LUMO (20) HOMO-4→LUMO+2 (13) HOMO-3→LUMO+2 (13)
10	3.474	357 (0.054)	HOMO-9→LUMO+1 (12)
11	3.564	348 (0.036)	HOMO-4→LUMO+3 (11) HOMO-1→LUMO+4 (14)
12	3.569	347 (0.017)	HOMO-1→LUMO+4 (52)
13	3.591	345 (0.014)	HOMO-5→LUMO+1 (7) HOMO-5→LUMO+2 (7)
14	3.636	341 (0.023)	HOMO-8→LUMO+2 (11) HOMO-3→LUMO+3 (11) HOMO-2→LUMO+4 (13)
15	3.697	335 (0.050)	HOMO-11→LUMO (13)
16	3.762	330 (0.025)	HOMO-6→LUMO+1 (12) HOMO→LUMO+5 (11)
17	3.793	327 (0.080)	326 HOMO-6→LUMO (11)
18	3.851	322 (0.027)	HOMO-7→LUMO (19) HOMO-4→LUMO+4 (12)
19	3.922	316 (0.038)	HOMO-7→LUMO (13) HOMO-6→LUMO+3 (28) HOMO→LUMO+5 (19)
20	3.997	310 (0.132)	HOMO-4→LUMO+4 (28)

[a]Oscillator strength greater than 0.010. [b]Components with greater than 10% contribution shown.

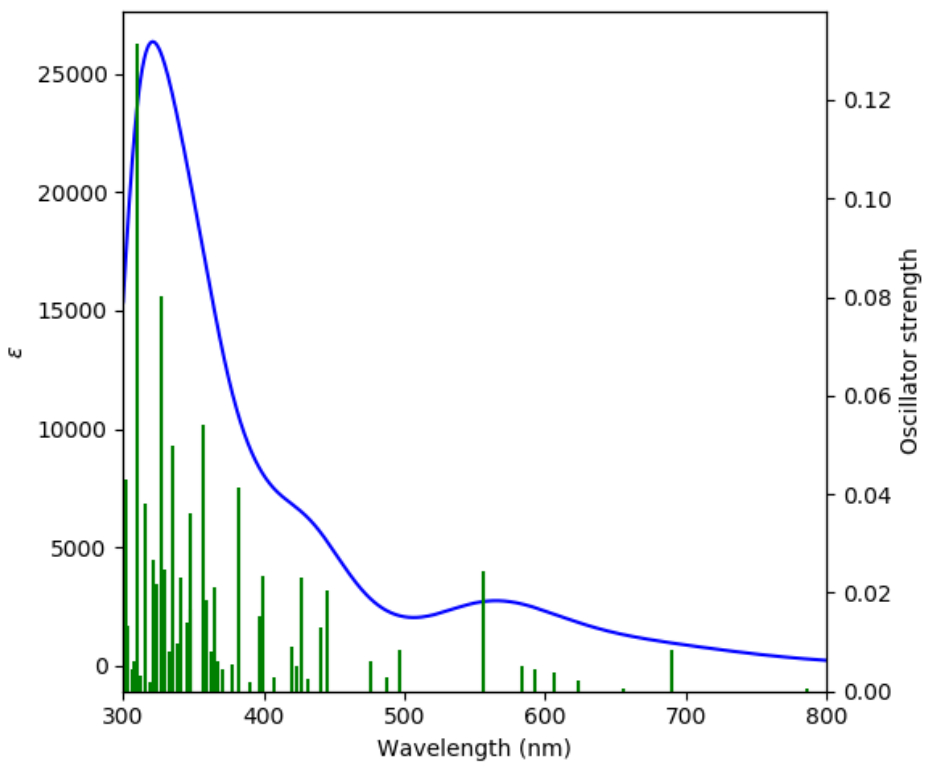


**Figure S9.** Absorption spectrum of **2** computed at the TD-DFT-B3LYP/Def2-TZVP level of theory ( $\epsilon$  in  $\text{LM}^{-1}\text{cm}^{-1}$ ).

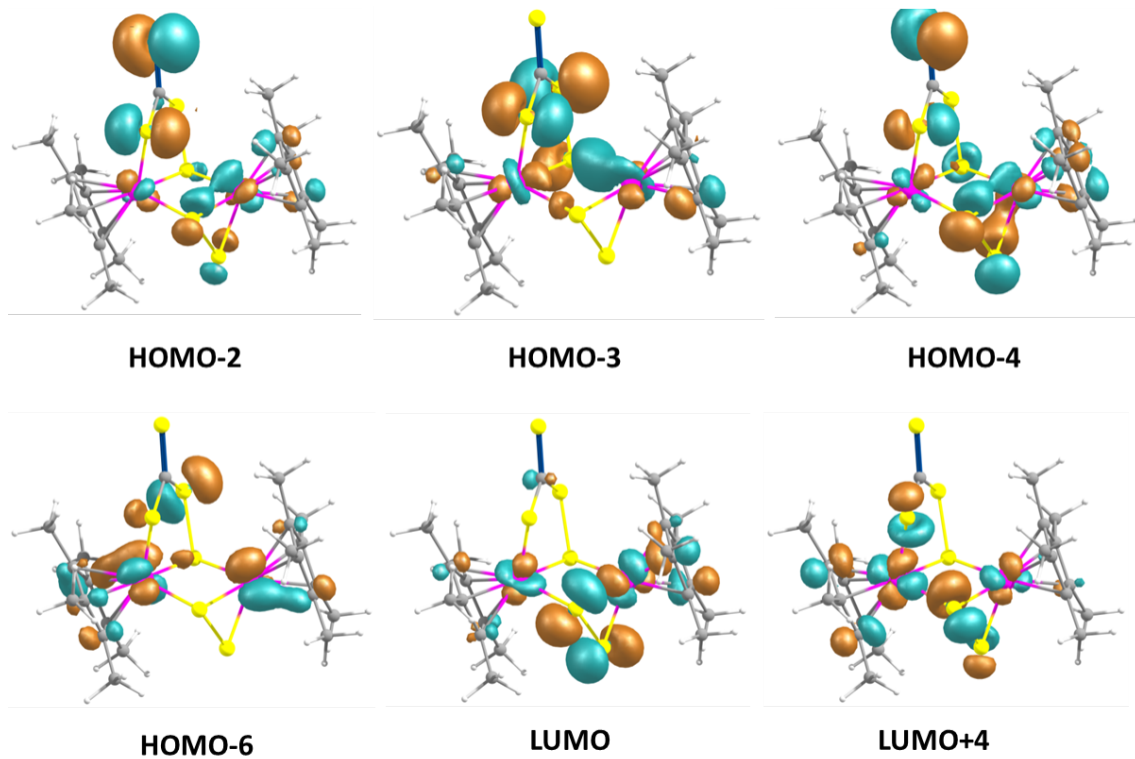


**Figure S10.** Selected molecular orbitals of **2** related to most intense electronic transitions [isocontour values:  $\pm 0.045$  ( $e/\text{bohr}^3)^{1/2}$ ].

### III. Cartesian Coordinates of the Optimized Structure 2

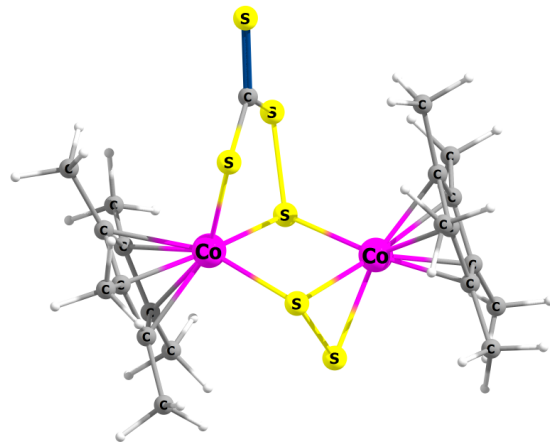


**Figure S11.** Optimized geometry of 2.

Total energy = -5973.76317959 a.u.

Cartesian coordinates for the calculated structure 2 (in Å)

C	3.704523000	0.020408000	-0.047484000	C	-3.038734000	0.428488000	-2.825436000
C	3.255758000	-0.402533000	1.223711000	H	-2.791096000	-0.514146000	-3.311409000
C	3.382592000	-1.011397000	-0.999181000	H	-2.243114000	1.138880000	-3.044879000
C	2.821446000	-2.111235000	-0.275436000	H	-3.957819000	0.806286000	-3.285136000
C	2.697027000	-1.726851000	1.085515000	C	-2.675028000	2.687650000	-0.636403000
C	2.217743000	-2.582802000	2.212717000	H	-3.590057000	3.250207000	-0.851743000
H	1.480667000	-3.310261000	1.878531000	H	-2.013562000	2.795473000	-1.494011000
H	1.755123000	-1.985537000	2.997688000	H	-2.189476000	3.162060000	0.212719000
H	3.056627000	-3.126610000	2.659910000	C	-3.377242000	1.433328000	2.212522000
C	3.410808000	0.333135000	2.515165000	H	-4.326158000	1.965278000	2.335745000
H	4.293930000	-0.028281000	3.051929000	H	-2.579776000	2.173695000	2.258069000
H	2.548955000	0.187090000	3.165675000	H	-3.263331000	0.761075000	3.062049000
H	3.531203000	1.403607000	2.359525000	C	-4.334703000	-1.572917000	1.751221000
C	4.441642000	1.282074000	-0.354121000	H	-3.898454000	-1.374531000	2.729432000
H	4.191271000	1.668222000	-1.340514000	H	-4.136263000	-2.614350000	1.502601000
H	5.520011000	1.093133000	-0.329936000	H	-5.419414000	-1.455906000	1.844586000
H	4.225339000	2.066294000	0.369249000	C	-4.104715000	-2.191051000	-1.378609000
C	3.740701000	-0.997003000	-2.451615000	H	-3.487824000	-2.398352000	-2.252476000
H	3.670175000	0.006803000	-2.869869000	H	-5.143975000	-2.119269000	-1.715851000
H	3.086266000	-1.645902000	-3.032902000	H	-4.024855000	-3.048733000	-0.713915000
H	4.767773000	-1.345277000	-2.602258000	C	0.839071000	2.767123000	-0.224145000
C	2.473200000	-3.447293000	-0.844934000	S	0.925652000	4.384660000	-0.549909000
H	3.340345000	-4.112454000	-0.781607000	S	0.276683000	2.344258000	1.395019000
H	2.185939000	-3.380996000	-1.893459000	S	1.246584000	1.519937000	-1.334152000
H	1.654745000	-3.917119000	-0.301822000	S	-0.017712000	0.264587000	1.384970000
C	-3.013547000	1.257860000	-0.367469000	S	-0.172519000	-1.334569000	-1.180692000
C	-3.370370000	0.693510000	0.914250000	S	-1.013811000	-2.543959000	0.254693000
C	-3.799733000	-0.643359000	0.708418000	Co	1.576181000	-0.368217000	-0.122772000
C	-3.692381000	-0.924823000	-0.700052000	Co	-1.806817000	-0.430483000	0.081385000
C	-3.233732000	0.258674000	-1.353192000				

## References

1. Kaur, U.; Saha, K.; Bairagi, S.; Das, A.; Roisnel, T.; Paine, T.K.; Ghosh, S. Structural and electronic analysis of bimetallic thiolate complexes of group-5 transition metal ions. *J. Organomet. Chem.* **2021**, *949*, 121943–121954.
2. Kaur, U.; Saha, K.; Raghavendra, B.; Ghosh, S. Role of Metals and Thiolate Ligands in the Structures and Electronic Properties of Group 5 Bimetallic–Thiolate Complexes. *Inorg. Chem.* **2020**, *59*, 12494–12503.
3. All pulse sequences are available in a commercial Bruker spectrometer.  $^1\text{H}$  decoupled  $^{11}\text{B}$  spectra were processed with backward linear prediction algorithm to remove broad  $^{11}\text{B}$  background signal from NMR probe and NMR tube.
4. Weiss, R.; Grimes, R.N. Sources of Line Width in Boron-11 Nuclear Magnetic Resonance Spectra. Scalar Relaxation and Boron-Boron Coupling in  $\text{B}_4\text{H}_{10}$  and  $\text{B}_5\text{H}_9$ . *J. Am. Chem. Soc.* **1978**, *100*, 1401–1405.
5. Led, J.J.; Gesmar, H. Application of the linear prediction method to NMR spectroscopy. *Chem. Rev.* **1991**, *91*, 1413–1426.